

# Single-molecule stochastic resonance

K. Hayashi<sup>1,2</sup>, S. de Lorenzo<sup>3</sup>, M. Manosas<sup>4</sup>, J. M. Huguet<sup>1</sup> and F. Ritort<sup>1,3,\*</sup>

1) *Departament de Física Fonamental, Facultat de Física, Universitat de Barcelona, Diagonal 647, E-08028, Barcelona, Spain*

2) *Department of Applied Physics, School of Engineering, Tohoku University, 2-1-1 Katahira, Sendai 980-8577, Miyagi, Japan.*

3) *CIBER de Bioingeniería, Biomateriales y Nanomedicina, Instituto de Salud Carlos III, Madrid, Spain*

4) *Laboratoire de Physique Statistique, Ecole Normale Supérieure, Unité Mixte de Recherche 8550 associée au Centre National de la Recherche Scientifique et aux Universités Paris VI et VII, 75231 Paris, France \**

(Dated: September 6, 2018)

Stochastic resonance (SR) is a well known phenomenon in dynamical systems. It consists of the amplification and optimization of the response of a system assisted by stochastic noise. Here we carry out the first experimental study of SR in single DNA hairpins which exhibit cooperatively folding/unfolding transitions under the action of an applied oscillating mechanical force with optical tweezers. By varying the frequency of the force oscillation, we investigated the folding/unfolding kinetics of DNA hairpins in a periodically driven bistable free-energy potential. We measured several SR quantifiers under varied conditions of the experimental setup such as trap stiffness and length of the molecular handles used for single-molecule manipulation. We find that the signal-to-noise ratio (SNR) of the spectral density of measured fluctuations in molecular extension of the DNA hairpins is a good quantifier of the SR. The frequency dependence of the SNR exhibits a peak at a frequency value given by the resonance matching condition. Finally, we carried out experiments in short hairpins that show how SR might be useful to enhance the detection of conformational molecular transitions of low SNR.

PACS numbers:

## I. INTRODUCTION

All nonlinear systems that exhibit stochastic noise are susceptible to undergo stochastic resonance (SR). When SR is triggered, the response of a system to an external forcing is amplified. SR has been studied in a large variety of systems, including climate dynamics [1, 2], colloidal particles [3–5], biological systems [6–8], and quantum systems [9, 10]. With the recent advent of single-molecule techniques, it is nowadays possible to measure SR at the level of individual molecules. Biomolecules exhibit rough and complex free energy landscapes that determine folding kinetics and influence the way they fold into their native structures. The use of force spectroscopy techniques has become important practice in studies of molecular biophysics. By applying a mechanical force at both extremities of an individual molecule and by recording the time evolution of the molecular extension (the reaction coordinate in these experiments), information about the folding reaction can be obtained. The application of forces makes possible to disrupt the weak bonds that hold their native structure to reach a stretched unfolded conformation. In this way thermodynamics (e.g. the free energy of folding) and kinetics (the rates of unfolding and folding) can be determined.

Although most SR studies use temperature as a tunable parameter, this is not the best choice to investigate

SR effects at the single-molecule level. Biomolecules have a strong sensitivity to temperature variations. Indeed, beyond increasing thermally assisted noise, temperature also modifies the shape of the molecular free energy landscape. Thus, another tunable parameter such as the oscillation frequency of force might be more appropriate to study SR in biomolecules. SR appears as a maximum in the response of a biomolecule at a characteristic frequency (the resonance frequency). This occurs when a characteristic timescale of the signal (e.g. its decorrelation or relaxation time) matches half period of the oscillation (the so-called matching condition). The matching condition must not be taken as a strict equality but a qualitative relationship between the two timescales [11, 12]. This means that different SR quantifiers may not give coincident resonance frequencies specially for low quality resonance peaks. It seems important to investigate which SR quantifier is best suited to identify SR behavior.

In this work, we use optical tweezers to investigate SR in single DNA hairpins driven by oscillatory mechanical forces. The high chemical stability of DNA makes DNA hairpins excellent models to investigate SR at the single-molecule level. When force oscillates around the average unfolding force, thermally activated hopping kinetics between the folded (F) and unfolded (U) states synchronizes with the frequency of the external driving force, leading to SR. SR can be measured by recording the oscillations produced in the molecular extension, relative to the magnitude of the noise produced by the thermal forces. Our aim in this work is to perform a systematic study of SR

---

\*Electronic address: fritort@gmail.com

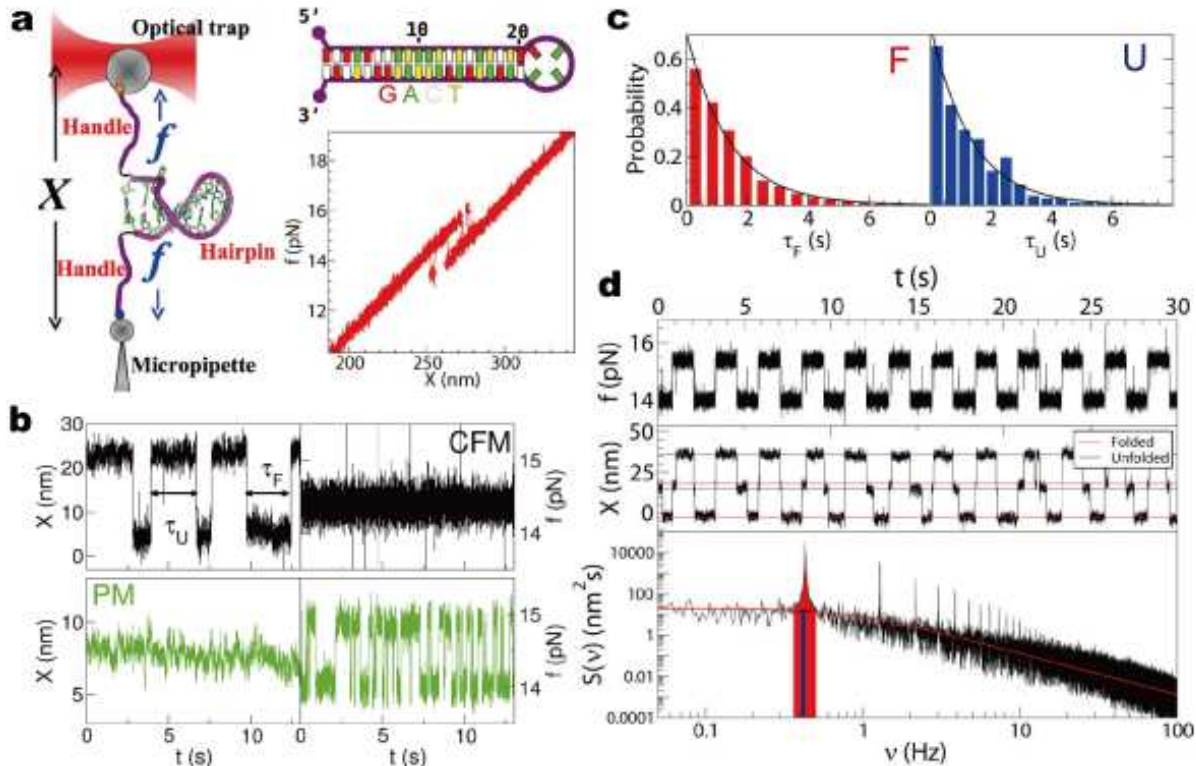


FIG. 1: **Experimental setup, hopping and SR experiments.** (a) Illustration of the experimental system (left), DNA sequence of the two-state hairpin H1 (upper right, sequence shown in color code) and experimental force-distance curve for H1 obtained from a pulling experiment (lower right). (b) Typical force and extension traces of the hopping experiments for H1 obtained in CFM (upper) and PM (lower). (c) Probability distributions of the residence times for H1 in the F (red) and U (blue) states obtained from the hopping experiments at  $f = f_c \simeq 14.5$  pN in the CFM. The black curves show the exponential fit,  $(1/a)\exp(-\tau/a)$ , to the data, with  $a=1.42$  s ( $a=1.34$  s) for the F (U) state. (d) Typical force and extension traces (upper and middle) obtained by applying a force oscillation protocol with amplitude  $A = 0.7$  pN and frequency  $\nu_{os} = 0.4$  Hz around the coexistence force  $f_c \simeq 14.5$  pN. In the lower panel, we show the measured power spectrum,  $S(\nu)$ , calculated by Fast Fourier Transform with window size  $N = 2^{17}$  of  $X(t)$  shown in the middle panel. The sampling rate of the instrument is 1 kHz. The red area is the output signal (OS, Eq.2) and the blue vertical bar represents the background noise (BN, Eq.3).

in single-molecules exhibiting bistable dynamics, rather than using SR as a useful tool to determine the kinetic properties of DNA hairpins. In fact, these can be estimated by using other much less time-consuming methods (e.g. by directly analyzing hopping traces). Yet, we also carry out SR studies in short hairpins that show how SR might prove useful to enhance the detection of conformational transitions of low SNR.

The paper is organized as follows. In Section II, our experimental set up is explained. Our main SR results in DNA hairpins are presented in Section III, and the influence of the experimental conditions (i.e. dsDNA handle length and trap stiffness) is investigated in Section IV. We compare different SR quantifiers in Section V and in section VI we describe the related phenomenon of resonant activation. Finally in Section VII, we purposely designed short DNA sequences to increase the noise of the signal to test whether SR can still be used to identify the hopping rate. In the last section, we summarize our conclusions, and discuss situations where SR might be a

useful technique.

## II. EXPERIMENTAL SETUP AND HOPPING EXPERIMENTS

In Fig. 1a, we show a schematic illustration of our experimental setup (left) and the DNA sequence of hairpin H1 that we investigated (upper right). The DNA hairpin is tethered between two short dsDNA handles (29 bp) that are linked to micron-size beads [13]. One bead is captured in the optical trap whereas the other is immobilized at the tip of a glass pipette [14]. By moving the position of the optical trap relative to the pipette, a force is exerted at the extremities of the hairpin.

In a pulling experiment, the optical trap is moved away from the pipette and mechanical force is applied to the ends of the DNA construct (DNA hairpin plus DNA handles) until the value of the force at which the hairpin unfolds is reached. In the reverse process, the trap ap-

proaches the pipette and the force is relaxed until the hairpin refolds. In this experiment, the force exerted upon the system,  $f$ , is recorded as a function of the relative trap-pipette distance giving the so-called force-distance curve (Fig. 1a, lower right). Around the co-existence force,  $f_c \simeq 14.5$  pN, the hairpin hops between the F and U states for sufficiently low pulling speeds.

Hopping experiments can be done in two different modes: constant force mode (CFM) and passive mode (PM) [15, 16]. In the CFM, the force applied to the DNA construct is maintained at a preset value by moving the optical trap through force-feedback control (Fig. 1b, upper). The folding and unfolding transitions of the DNA hairpin are followed by recording the trap position,  $X(t)$ . In contrast to the CFM, the PM is operated by leaving the position of the optical trap stationary without any feedback. The bead passively moves in the trap in response to changes in the extension of the DNA construct (Fig. 1b, lower). When the hairpin unfolds, the trapped bead moves toward the trap center and the force decreases; when the hairpin folds, the trapped bead is pulled away from the trap center and the force increases. The folding and unfolding transitions of the DNA hairpin are followed by recording the force,  $f(t)$ . In both cases (CFM and PM), the kinetic rates of hopping can be measured from the residence times of the trace ( $X(t)$  in the CFM and  $f(t)$  in the PM). Fig. 1b shows hopping traces measured in the CFM and PM at the co-existence force,  $f_c \simeq 14.5$  pN, where the hairpin hops between the F and U states populating them with equal probability (i.e. it spends equal time in both states).

In this work, we focused on the experiments at controlled force, rather than at fixed trap position. Both the hopping and the oscillation experiments (described below) were carried out using the force feedback control. The reason is that the controlled force experiments avoid undesirable drift effects in force that strongly affect the kinetics of the hairpin (see Methods). Therefore we mainly carried out the experiments in the CFM by recording the position of the trap,  $X(t)$ . This signal exhibits dichotomic motion between the two distinct levels of extension (Fig. 1b, upper left). The difference between the two levels (short extension, folded; long extension, unfolded) reflects the release in extension ( $\simeq 18$  nm) of the 44 nucleotides of hairpin H1. From  $X(t)$  we can extract the residence time distribution at each state that shows the exponential form characteristic of first-order decay processes (Fig. 1c). The fit of the time distribution to an exponential function allow us to get the average residence time. The force-dependent kinetic rates (equal to the inverse of the mean lifetimes),  $k_{FU}$  and  $k_{UF}$ , were measured at the co-existence force,  $f_c = 14.5 \pm 0.3$  pN, giving  $k_c = k_{FU}^c = k_{UF}^c \simeq 0.66 \pm 0.04$  s $^{-1}$  (Table S0 in SI).

### III. SR EXPERIMENTS

To induce the SR phenomenon, we applied an oscillating force,  $f(t)$ , to the DNA hairpin using the force feedback protocol, where  $f(t) = f_c + f_{os}(t)$ . For  $f_{os}(t)$  we chose a square-wave signal of amplitude,  $A$ , and frequency,  $\nu_{os} = 1/T_{os}$ , where  $T_{os}$  is the oscillation period (Fig. 1d, upper). The four distinct levels of extension observed (Fig. 1d, middle) correspond to the molecular extensions of the hairpin in the F and U states at the two force values,  $f = f_c + A$  and  $f = f_c - A$ . The power spectral density,  $S(\nu)$ , is defined as the Fourier transform of the stationary correlation function of the signal  $X(t)$ :

$$S(\nu) = \int_{-\infty}^{+\infty} dt \langle X(t)X(0) \rangle e^{-i2\pi\nu t}, \quad (1)$$

where  $\langle \cdot \rangle$  denotes a time-average over the signal. As shown in Fig. 1d (lower),  $S(\nu)$  can be described as the superposition of a background power spectral density,  $S_N(\nu)$ , and a structure of delta spikes centered at  $\nu_n = (2n+1)\nu_{os}$  ( $n = 0, 1, 2, \dots$ ). In order to extract the signal from the background noise, we define the output signal (OS), the background noise (BN) and the signal-to-noise ratio (SNR) as [11],

$$\text{OS} = \lim_{\Delta\nu \rightarrow 0} \int_{\nu_{os}-\Delta\nu}^{\nu_{os}+\Delta\nu} S(\nu) d\nu. \quad (2)$$

$$\text{BN} = S_N(\nu_{os}). \quad (3)$$

$$\text{SNR} = \frac{\text{OS}}{\text{BN}} = \frac{1}{S_N(\nu_{os})} \lim_{\Delta\nu \rightarrow 0} \int_{\nu_{os}-\Delta\nu}^{\nu_{os}+\Delta\nu} S(\nu) d\nu. \quad (4)$$

The SNR defined in Eq.(4) is equal to the ratio of the spectral power of the signal at the frequency  $\nu_{os}$  (OS), to the noise-floor spectral density measured in the presence of the oscillation (BN) and has dimensions of Hz. Fig. 1d (lower) illustrates how we measured the OS (red area) and the BN (blue vertical bar) from the spectral density. Other equivalent definitions of the SNR [17] are the dimensionless ratio between the power in the output signal (Eq.(2)) and the total input noise power delivered by the noise (proportional to the integral of background spectral density  $S_N(\nu)$  over all  $\nu$ ). Because the total input noise power only depends weakly on  $\nu_{os}$ , we can take the OS, Eq.(2), as another indicator of the SR phenomenon. Indeed, both indicators OS and SNR are equally valid to identify resonant behavior, even though the peak is often more visible in the latter (see below) [18].

For the hairpin H1 at high trap power and trap stiffness  $\kappa_{\text{trap}} \simeq 70$  pN/ $\mu\text{m}$ , the resulting OS and BN as a function of  $\nu_{os}$  are depicted in Fig. 2a (lower), while Fig. 2c shows the SNR. In contrast to the OS, the presence of a peak around  $\nu_{os} = 0.4 \pm 0.05$  Hz is apparent for the SNR. This value is close to that predicted by the matching condition,  $\nu_{SR} = k_c/2$ , which states that the SNR is maximum when the average hopping time of the hairpin ( $1/k_c = 1.56$  s) is equal to half the period of the forcing oscillation ( $1/2\nu_{os} = 1.25$  s) [11, 19–21]. This

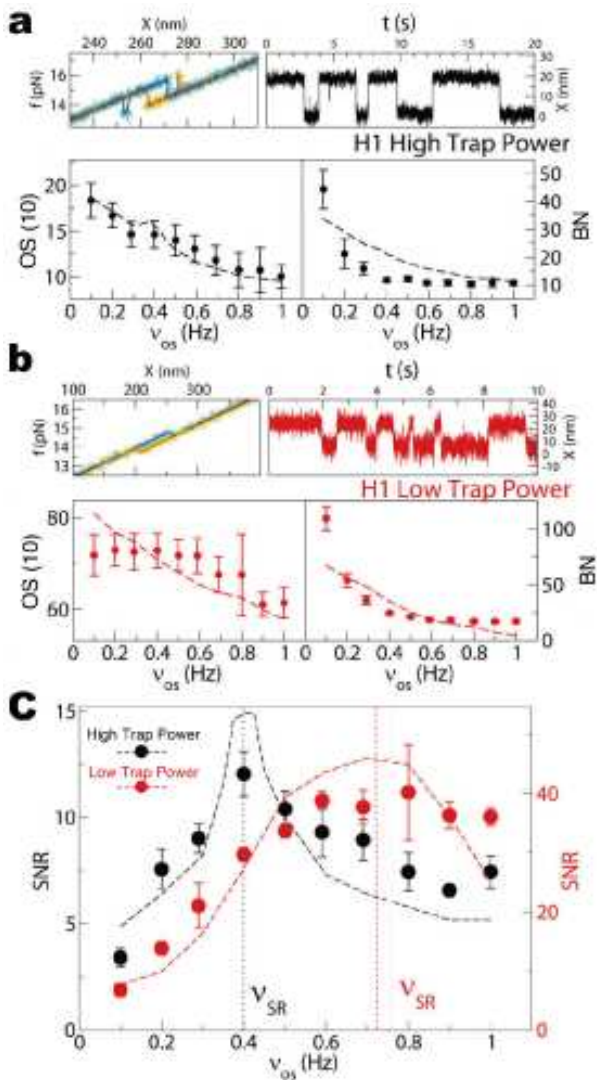


FIG. 2: **SR experiments for hairpin H1 at different trap stiffness.** Pulling cycle (unfolding, blue; refolding, red), hopping trace, OS and BN for H1 with amplitude  $A = 0.7$  pN at high trap stiffness,  $\kappa_{\text{trap}} = 70$  pN/ $\mu\text{m}$  (a), and at low trap stiffness,  $\kappa_{\text{trap}} = 24$  pN/ $\mu\text{m}$  (b). Results averaged over 5-10 molecules. (Note: the force rips shown in force-distance curves should drop vertically without any finite stiffness correction. The finite slope correction shown in Fig. 2b (top, left) is due to low-bandwidth filtering of data). (c) SNR at high trap stiffness (low trap power) depicted in black (red). Units: OS ( $\text{nm}^2$ ), BN ( $\text{nm}^2/\text{Hz}$ ), SNR (Hz). Simulation results are shown as dashed lines (Figs. S4 and S7 in SI). The error bars represent the standard error over different molecules.

shows that SR in single-molecule hopping experiments approximately fulfills the matching condition as has been observed in other bistable systems.

The OS and the SNR can be calculated theoretically as a function of the oscillation frequency for a Brownian particle in a continuous double-well potential [18, 19, 22]. In this model, the OS and the SNR exhibit a soft and

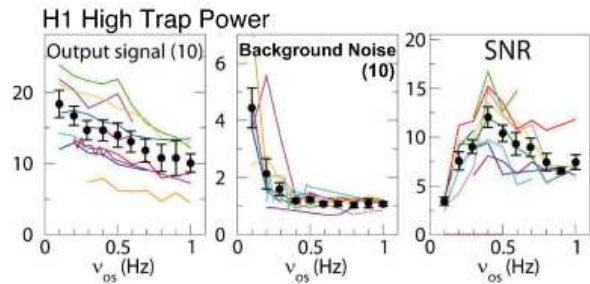


FIG. 3: **Molecular variability of the measured responses (H1).** Results for the OS, BN and SNR for 10 different molecules at high trap power  $\kappa_{\text{trap}} = 70$  pN/ $\mu\text{m}$ . Units: OS ( $\text{nm}^2$ ), BN ( $\text{nm}^2/\text{Hz}$ ), SNR (Hz). The error bars represent the standard error over different molecules.

a sharp peak, respectively, only when SR is induced at large enough forcing amplitudes [18]. These large forcing amplitudes correspond to a non-linear regime of the system, in which the shape of the double-well potential is so deformed that the barrier separating the wells vanishes at the maximum elongation of the oscillation. In our experiments, we applied a large oscillation amplitude ( $A=0.7$  pN). Note that the region of coexistence between the F and U states spans less than 3 pN in Fig. 1a (lower right). Thus an extra-force of 0.7 pN strongly alters the barrier and the relative free energy between states F and U. Our experimental results agree with the theoretical predictions by Stocks [18] obtained in the non-linear response regime. We performed a numerical simulation of an overdamped particle moving in a double-well potential with parameters that fit the experimentally measured molecular free energy landscape (Sec. IV in SI). Despite its simplicity, the model qualitatively reproduced the experimental results for the OS, BN and SNR (dashed lines in Fig. 2c).

In order to see what happens for lower oscillation amplitudes, we explored the response of hairpin H1 to an oscillating force of lower amplitude,  $A = 0.2$  pN. A very soft peak and a gentle maximum in the OS and the SNR can be seen around 0.4 Hz (Fig. S1 in SI) in agreement with the results previously obtained for the higher amplitude,  $A = 0.7$  pN (Fig. 2). However, the peak for  $A = 0.2$  pN is much less clear than the peak for  $A = 0.7$  pN, showing the importance of using oscillation amplitudes beyond the linear-response regime ( $AX^{\ddagger}/k_B T \ll 1$ , where  $X^{\ddagger}$  is the characteristic distance separating the folded or unfolded states from the transition state. See also Sec. III in SI for SR behavior in the linear response regime).

A characteristic feature of SR experiments at the single-molecule level is the large variability observed in the measured response from different molecules. Fig. 3 shows the OS, BN and SNR for 10 different molecules. Larger variability is observed for the OS as compared to the BN. This might be due to non-linear effects which are

sensitive to small differences in the experimental setup (e.g. tether misalignment with respect to the pulling direction, variations in the size of the bead and the trap stiffness, etc.).

#### IV. INFLUENCE OF TRAP STIFFNESS AND LENGTH OF THE HANDLES

An important issue in single-molecule experiments concerns the influence of transducing effects induced by the experimental setup (e.g. trap stiffness and length of the handles) on the measured kinetics. Recent studies [13, 15, 16] show that the kinetic rates are only moderately affected (within one order of magnitude) when changing the length of the handles one thousand-fold or the trap stiffness ten-fold. Besides, numerical simulations carried out in Ref. [16] show that kinetic rates for hairpins measured with handles and trap always remain close and converge to the intrinsic rate (i.e. the rate measured without handles and trap) in the limit of very compliant linkers. To inquire the influence of the experimental design on the kinetics of hairpin H1, SR was further investigated by varying conditions of the experimental setup such as 1) the stiffness of the optical trap and 2) the length of the handles. We observed how both effects changed the intrinsic noise of the system (Figs. 2b, 2c and 4). In the first case, when the trap stiffness,  $\kappa_{\text{trap}}$ , was decreased from 70 pN/ $\mu\text{m}$  to 24 pN/ $\mu\text{m}$  (Fig. 2b), the maximum peak in the SNR was shifted to higher frequencies (from 0.4 Hz to  $\simeq 0.8$  Hz) and became less clear (Fig. 2c, red curve). The effect of the trap stiffness on SR was evaluated by using the numerical simulation (Sec. IV in SI), finding good agreement between experiments and simulations (Figs. 2b and 2c).

In the second case, if we increase by twenty-fold the length of the handles (528 bp and 874 bp at each flanking side) keeping the trap stiffness constant,  $\kappa_{\text{trap}} = 70$  pN/ $\mu\text{m}$ , we find that the resonance frequency shifts to a larger value for the long handles (Fig. 4). For the long handle construct, the matching condition is verified ( $\nu_{\text{SR}} = 2$  Hz) and  $k_c \simeq 4$  s $^{-1}$  as obtained from hopping experiments [13].

The dependence of the resonance frequency measured from SR,  $\nu_{\text{SR}}$ , on the trap stiffness and the length of the handles was similar to that reported for the hopping rate measured in the hopping experiments at the co-existence force [13, 15, 16]. In both cases, the soft trap stiffness or the larger compliance of the long handles contributes to increase the hopping rate, supporting the conclusions of Ref. [13]. Interestingly enough, the quality of the resonant peak worsens as the trap stiffness decreases but not as the linker becomes softer, showing that the quality of the SR peak is only dependent on the combined effective stiffness of bead and handles ( $\kappa_{\text{eff}}^{-1} = \kappa_{\text{trap}}^{-1} + \kappa_{\text{handle}}^{-1} \simeq \kappa_{\text{trap}}^{-1}$ ) which is approximately equal to the trap stiffness in our experimental conditions.

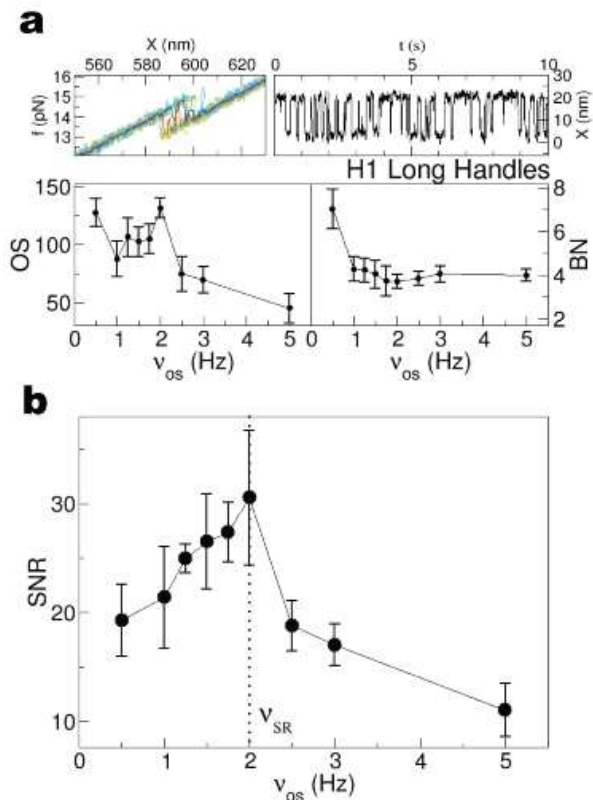


FIG. 4: **SR experiments for hairpin H1 with long DNA handles.** (a) Pulling cycle (unfolding, blue; refolding, red), hopping trace, OS and BN depicted in violet. (b) The resulting SNR in the case of high trap stiffness  $\kappa_{\text{trap}} = 70$  pN/ $\mu\text{m}$  and the amplitude  $A = 0.7$  pN. Results averaged over 5 molecules. Units: OS (nm<sup>2</sup>), BN (nm<sup>2</sup>/Hz), SNR (Hz). The error bars represent the standard errors over different molecules.

#### V. OTHER SR QUANTIFIERS

Next we investigated other representative SR quantifiers. These are: the fraction  $P_1$  of transitions that occur every half-period of the oscillation [4, 23, 24]; and the average dissipated work,  $W$  [5, 25]. To extract  $P_1$ , we measured the residence time distributions,  $P(\tau_{\text{F}})$  and  $P(\tau_{\text{U}})$ , of the F and U states in the presence of the oscillating force. The distributions are shown in Fig. 5a for hairpin H1 in the cases  $\nu_{\text{os}} = 0.4$  Hz (upper) and  $\nu_{\text{os}} = 5$  Hz (lower) with  $A=0.7$  pN. Unlike the distributions shown in Fig. 1c,  $P(\tau_{\text{F}})$  ( $P(\tau_{\text{U}})$ ) is not monotonically decreasing with  $\tau_{\text{F}}$  ( $\tau_{\text{U}}$ ) and exhibits spikes corresponding to higher harmonics for  $\tau_{\text{F}} = T_{\text{os}}(1 + 2n)/2$  ( $\tau_{\text{U}} = T_{\text{os}}(1 + 2n)/2$ ) where  $n = 0, 1, 2, \dots$ . A few harmonic frequencies are shown as vertical arrows in Fig. 5a. In particular when  $\nu_{\text{os}}$  is close to the resonance frequency, the shape of the residence time distribution strongly deviates from an exponential and a broad peak appears around the fundamental mode,  $\tau_{\text{F}} = T_{\text{os}}/2$  ( $\tau_{\text{U}} = T_{\text{os}}/2$ ) (Fig. 5a, top). In

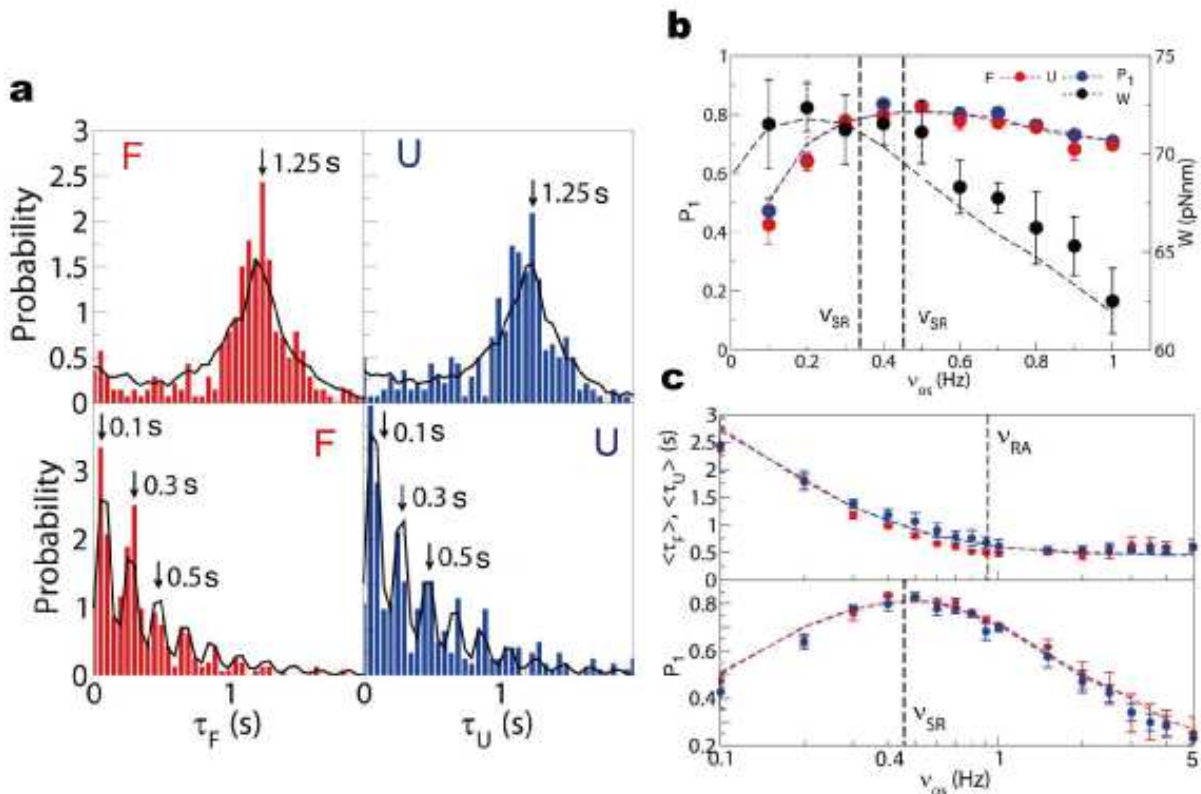


FIG. 5: **Other SR quantifiers in hairpin H1.** (a) Residence time distributions for the F (red) and U (blue) states at  $\nu_{os} = 0.4$  Hz (upper) and  $\nu_{os} = 5$  Hz (lower). The continuous black lines are the results of the simulations (Sec. IV in SI). (b)  $P_1$  in the F (red) and U (blue) and average work  $W$  (black) as a function of input frequency. Simulation results are shown by the dashed lines (Sec. IV in SI). Vertical dotted line shows the expected resonance frequency. The maximum in  $P_1$  is broad around 0.3-0.6 Hz, while that in  $W$  is also broad with a maximum found at a lower frequency in the range 0.1-0.4 Hz. (c) Average residence times (upper panel) and  $P_1$  (lower panel) in the F (red) and U (blue) states as a function of input frequency. Note that the frequency range is larger than that shown in b). Simulation results are shown as dashed continuous lines (Sec. IV in SI). The vertical lines show the two frequencies characteristic of stochastic resonance ( $\nu_{SR}$ ) and resonant activation ( $\nu_{RA}$ ). Statistics: 8 molecules, 3-5 minutes traces and 300-600 hopping transitions at each input frequency. The error bars represent the standard errors over different molecules.

contrast, many peaks appear in the residence time distribution when  $\nu_{os} \gg \nu_{SR}$  (Fig. 5a, lower).

$P_1$  can be extracted from the area of the residence time distribution around the peak located at the fundamental mode,  $\tau_F = T_{os}/2$  ( $\tau_U = T_{os}/2$ ). Let  $\{\tau_i; i = 1, \dots, N\}$  be the series of  $N$  residence times measured in the presence of the oscillating force. By counting the number,  $n$ , of  $\tau_i$  that satisfy the condition  $T_{os}/2 - T_{os}/4 \leq \tau_i \leq T_{os}/2 + T_{os}/4$ , we define

$$P_1 = \frac{n}{N}. \quad (5)$$

$P_1$  takes a large value if the residence time of the hairpin is equal to half the period of the oscillating force. This means that a large fraction of hopping transitions occur when the oscillating force changes sign. Therefore, the value of  $P_1$  has a maximum when SR is induced, because the transitions between the two states are synchronized with the oscillating force ( $P_1$  is a *bona fide* SR quantifier

[23]. See also Sec. III in SI). The results obtained for  $P_1$  in hairpin H1 are shown in Fig. 5b.  $P_1$  exhibits a broad maximum around the resonance value  $\nu_{SR} = k_c/2 = 0.4$  Hz. The broadness of the peak is in contrast to the narrower peak observed in the SNR (Fig. 2c). These results are consistent with analytical calculations [11, 23].

For the average cyclic work done by an oscillating force, we define [26]

$$W = -\langle \oint X df \rangle = \langle \oint f dX \rangle, \quad (6)$$

where the brackets stand for statistical averages over traces. Because  $W$  takes a large value when the folding/unfolding of the hairpin is synchronized with the oscillating force, it is a useful SR quantifier as well [5, 27]. In fact, the larger the synchronisation between transitions of the hairpin and oscillations in the force, the larger the work done by the optical trap on the molecule. Re-

sults for  $W$  are shown in Fig. 5b. In contrast to SNR but similarly to  $P_1$ , the maximum in  $W$  is broad. Finally, we compared our experimental results with the predictions obtained from the numerical simulations in the continuous double-well potential whose parameters are the same as those used in Fig. 2 (Sec. IV in SI). Figs. 5a and 5b show a good agreement between experiments and simulations. Although both  $P_1$  and  $W$  show broad maxima as a function of  $\nu_{os}$ , they are not coincident, the maximum for the work is found at a lower frequency as compared to  $P_1$ . As pointed out in the introduction, the precise value of the resonance frequency depends on the quantifier specially when the quality of the resonant peak is low.

## VI. RESONANT ACTIVATION

In stochastic systems driven by oscillating forces, it is customary to distinguish two effects: stochastic resonance (SR) and resonant activation (RA). SR stands for the optimization of the response of the system (i.e. the output signal) whereas RA stands for the optimization of kinetics (i.e., maximization of the number of hopping transitions per second). SR and RA are different phenomena related to barrier crossing dynamics along temporally modulated energy landscapes [4]. RA is induced when the mean residence times of the states of the system are minimized with respect to the frequency of the oscillating force,  $\nu_{RA}$ . The values of  $\nu_{SR}$  and  $\nu_{RA}$  are often not the same, the latter being typically larger than the former. Fig. 5c (top) shows the mean residence times,  $\langle\tau_F\rangle$  and  $\langle\tau_U\rangle$ , for hairpin H1 measured in the range  $0.1 \text{ Hz} \leq \nu_{os} \leq 5 \text{ Hz}$ . Only at higher frequencies (between 1 Hz and 2 Hz), the graph suggests a very shallow minimum for the residence times. Therefore we are capable of observing both the SR and RA phenomena in the single-molecule experiments. The experimental results also agree with the numerical simulations (Fig. 5c, dashed lines). Similar behavior has been reported in the experiments with a colloidal particle in a double-well potential generated by optical tweezers [4].

## VII. SR IN SHORTER HAIRPINS

SR might be used to detect the transitions in cases where the hoppings of a hairpin is hard to be discriminated. These correspond to cases in which the hopping signal (extension jumps) are on the same order of the standard deviation of noise fluctuations. To investigate this problem, we designed two short hairpins (SH10 and SH8) having only 10 and 8 base pairs along the stem, respectively (sequences shown in Figs. 6c and 6d). The molecular free energy landscapes were calculated for the two sequences at the theoretically predicted co-existence forces using the nearest-neighbour model for DNA (Fig. 6a, upper left) [28, 29]. As the length of the

stem decreases, the landscapes show progressively lower co-existence force values, molecular extensions and kinetic barriers. Measurements for SH10 and SH8 were taken at low trap stiffnesses to decrease the hopping signal ( $\kappa_{\text{trap}} \simeq 32 \text{ pN}/\mu\text{m}$  and  $17 \text{ pN}/\mu\text{m}$ , respectively). Pulling curves and hopping traces in the CFM are also shown in Fig. 6a (lower left). While the transitions are still visible for SH10, these are hardly discriminated for SH8. This is also apparent from the dwell distributions on trap position,  $X$ , shown in Fig. 6a (right). Measured jumps in the molecular extension upon unfolding/folding are equal to  $10.5 \pm 0.5 \text{ nm}$  and  $7.0 \pm 0.5 \text{ nm}$  for SH10 and SH8, respectively.

Fig. 6b shows the power spectra of  $X(t)$ . Whereas SH10 can be fit reasonably well to a sum of two Lorentzians with two characteristic corner frequencies ( $0.64 \pm 0.02 \text{ Hz}$  and  $2.4 \pm 0.3 \text{ kHz}$ ), the quality of the fit considerably worsens for SH8 ( $\simeq 9.8 \text{ Hz}$  and  $\simeq 15.6 \text{ kHz}$ ). The low frequency (in the range of Hz) in the power spectra corresponds to the hopping kinetics of the hairpin whereas the high frequency (in the range of kHz) corresponds to the random motion of the optical trap caused by the force feedback. Because the noise in the trap position,  $X$ , introduced by the force feedback protocol is not of thermal origin, the power spectra measured in the CFM should not necessarily be fit to a sum of two Lorentzians. This is specially acute for SH8 where the feedback loop cannot follow the fast hopping transitions.

Once the hopping properties of the hairpins were characterized, we then carried out the oscillating experiments for hairpins SH10 and SH8 around the co-existence force. The results we obtained for SH10 are similar to those reported for hairpin H1 at low trap power shown in Fig. 2c. For SH10 the peak in the SNR around  $\nu_{SR} = 0.5 \text{ Hz}$  is close to  $k_c/2$  where  $k_c$  was measured to be  $0.43 \pm 0.07 \text{ s}^{-1}$  from the hopping traces for  $X(t)$ . More interesting is the case of hairpin SH8 where the co-existence force can still be located, but the hopping signal is blurred by the fluctuations. In Fig. 6d, we can see that the OS and the SNR exhibit a maximum around  $\nu_{SR} = 5 \pm 1 \text{ Hz}$  for SH8 which gives  $k_c \simeq 10 \pm 2 \text{ s}^{-1}$  according to the matching condition. This value agrees with the value of  $\simeq 9.8 \text{ Hz}$  obtained from the Lorentzian fit to the power spectrum. As an additional test, we have implemented a Hidden Markov Model (HMM) with the forward-backward feedback algorithm as described in Ref. [30] to extract the kinetic rates of SH8 from the hopping trace,  $X(t)$ . By applying the HMM to the hopping traces of SH8, we obtained a value of  $k_c = 9.4 \pm 0.5 \text{ s}^{-1}$  (7 molecules), which confirms the results obtained with SR and Lorentzian fit to the spectral density.

Thus, SR offers an alternative method to estimate the hopping rate of SH8. Indeed, the two states (F and U) cannot be easily detected from the hopping trace and the residence time analysis done for hairpin H1 (Fig. 1c) is difficult to implement. In this case SR confirms the value of the hopping frequency initially obtained from a poor

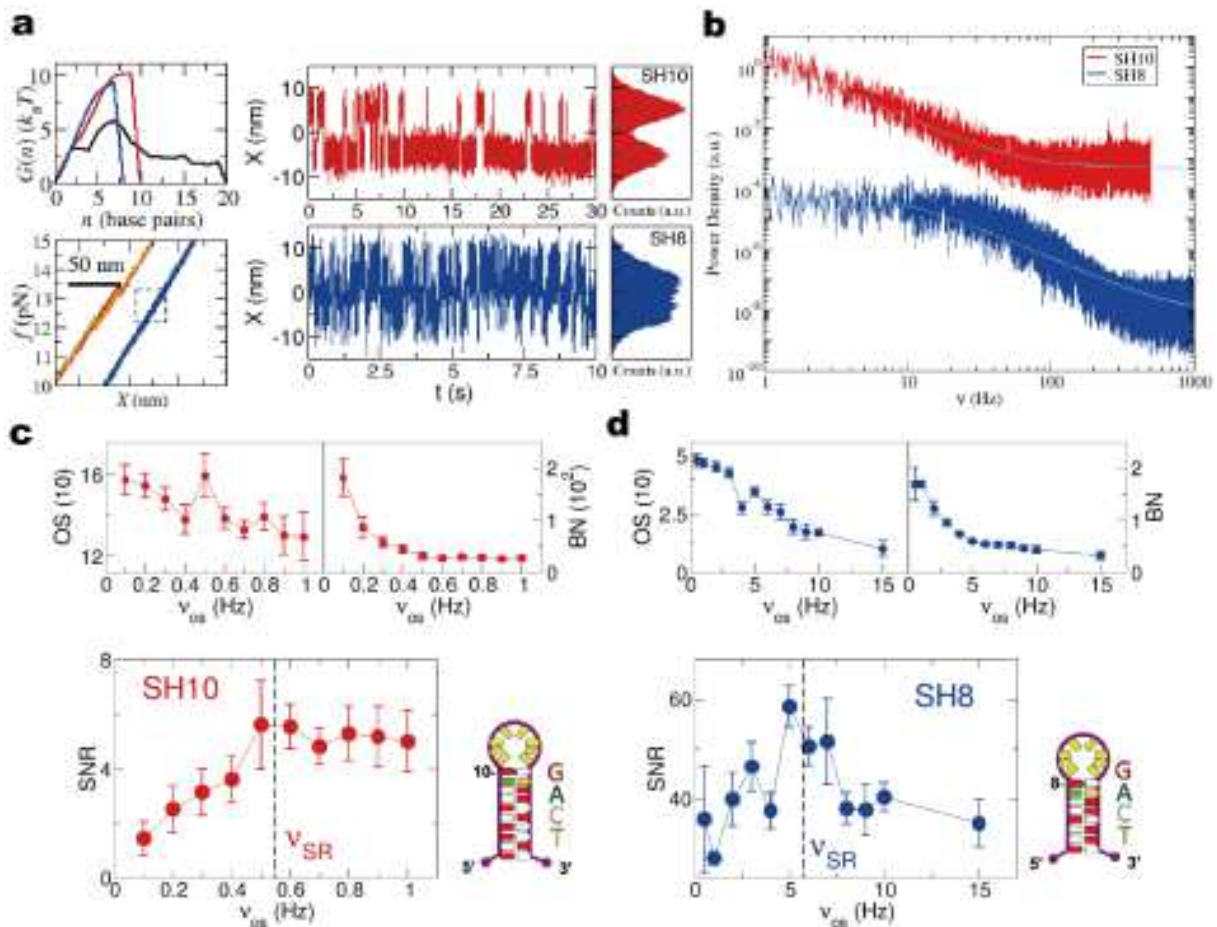


FIG. 6: **SR experiments in shorter hairpins.** (a) Free energy landscapes (upper left), force-distance curves (lower left) and hopping traces in the CFM for SH10 (red), SH8 (blue) and H1 (black). Measurements were carried out with a low trap power  $\kappa_{\text{trap}} \simeq 32$  pN/ $\mu\text{m}$  for SH10, 17 pN/ $\mu\text{m}$  for SH8, respectively. For sake of simplicity, all pulling curves in the lower left panel are shown parallel with equal average slopes. The dashed-squared region for SH8 curves indicates the region where unfolding/folding transitions occur. Distributions of trap position,  $X$ , show clear transitions for SH10 but not for SH8. (b) Power spectrum for SH10 and SH8. Cyan curves are fits to a sum of two Lorentzians (see text for details). Colors as in Fig. 6a. (c, d) OS, BN and SNR for SH10 and SH8. The amplitudes of oscillation force are  $A = 0.5$  pN for SH10 and  $A = 0.15$  pN for SH8, respectively. Colors as in Fig. 6a. Statistics (SH10, SH8): Molecules (5, 7); Duration of hopping traces (4, 2) minutes; Average number of hopping transitions (250, 1200) at each input frequency. Units: OS ( $\text{nm}^2$ ), BN ( $\text{nm}^2/\text{Hz}$ ), SNR (Hz). The error bars represent the standard errors over different molecules.

Lorentzian fit of the power spectrum.

## VIII. CONCLUSION

We carried out SR experiments in single DNA hairpins subject to an oscillatory mechanical force of varying frequency. Our aim was to investigate how a molecule exhibiting bistability (i.e. hopping between the folded and unfolded conformations) responds to an applied oscillating force. In SR the response gets amplified at frequencies close to the characteristic hopping frequency of the hairpin. By measuring the power spectral density of the molecular extension, we carried out a detailed in-

vestigation of the frequency dependence of the output signal (OS, Eq. (2)), the background noise (BN, Eq. (3)) and the signal-to-noise ratio (SNR, Eq. (4)) in the 20bp hairpin H1 which exhibits dichotomous hopping behavior. We then extended our research by exploring how several parameters of the experimental setup such as trap stiffness, length of the handles, oscillating amplitude and size of the hairpin influence the resonance behavior. From the measured traces, we also analyzed a few other SR quantifiers such as the number of folding and unfolding transitions occurring every half-period of the oscillation ( $P_1$ , Eq. (5)), the average mechanical work per period of the oscillation ( $W$ , Eq. (6)) and the mean residence times in the unfolded and folded states ( $\langle\tau_U$

**Comparison between  $\nu_{\text{SR}}$  (Hz) and  $k_c$  ( $\text{s}^{-1}$ )**

	$\nu_{\text{SR}}$ from SNR	$\nu_{\text{SR}}$ from OS	$\nu_{\text{SR}}$ from $P_1$	$\nu_{\text{SR}}$ from $W$	$k_c/2$
H1 <sup>a,c</sup>	$0.40 \pm 0.02$ ( $n = 10$ )	$0.45 \pm 0.03$ ( $n = 10$ )	$0.45 \pm 0.04^e, 0.48 \pm 0.08^f$ ( $n = 8$ )	$0.33 \pm 0.07$ ( $n = 8$ )	$0.33 \pm 0.02$ ( $n = 12$ )
H1 <sup>a,d</sup>	$0.72 \pm 0.08$ ( $n = 5$ )	$0.50 \pm 0.06$ ( $n = 5$ )	-	-	$0.53 \pm 0.07$ ( $n = 8$ )
H1 <sup>b,c</sup>	$2.0 \pm 0.2$ ( $n = 5$ )	$1.9 \pm 0.1$ ( $n = 5$ )	-	-	$2.2 \pm 0.3$ ( $n = 5$ )
SH10	$0.54 \pm 0.02$ ( $n = 5$ )	$0.58 \pm 0.04$ ( $n = 5$ )	-	-	$0.43 \pm 0.07$ ( $n = 4$ )
SH8	$5.7 \pm 0.4$ ( $n = 7$ )	$5.3 \pm 0.2$ ( $n = 7$ )	-	-	$4.7 \pm 0.3^g$ ( $n = 7$ )

TABLE I: Resonance frequency,  $\nu_{\text{SR}}$ , obtained from SNR, OS,  $P_1$  and  $W$  vs. hopping rate,  $k_c$ , at the co-existence force (see Sec. I in SI for  $k_c$ ).  $\nu_{\text{SR}}$  was chosen as the peak value of each SR quantifier for each molecule. (a. Short handles. b. Long handles. c. High power trap ( $\kappa = 70$  pN/ $\mu\text{m}$ ). d. Low power trap ( $\kappa = 24$  pN/ $\mu\text{m}$ ). e. Folded state. f. Unfolded state. g. Rate determined using a Hidden Markov Model (HMM). Note that  $n$  is the number of molecules analyzed.)

and  $\langle \tau_{\text{F}} \rangle$ ). The mean residence times describe a mechanism slightly different from SR that has been termed resonant activation (RA). Overall, we find that the SNR and the other SR quantifiers (such as OS,  $P_1$ ,  $W$ ) exhibit a peak at a frequency close to that determined by the resonance matching condition. Among all quantifiers only the SNR and the OS tend to show a modest amplification of the response, the SNR showing a higher quality peak. Our results are summarized in Table I. Moreover, our experimental results are well predicted by numerical simulations of an overdamped particle in a double-well potential reproducing the measured molecular free energy landscape of the hairpin (Sec. IV in SI). Finally, our experimental findings also agree with theoretical results [18] that show a modest gain in the response of noisy systems driven by oscillating forces.

A unique aspect of our work is the investigation of SR in small systems in conditions of weak thermodynamic stability (folding free energies of a few  $k_{\text{B}}T$  units) not far from noise level ( $k_{\text{B}}T$ ). This has a primary consequence: the proper control parameter in our experiments does not appear to be the noise intensity. In fact, by changing noise intensity (e.g. by tuning temperature or denaturant concentration), we also modify the structural properties of the molecule in a non-controlled way (i.e. by changing its thermodynamic stability or free energy of formation). Our work circumvents this problem by using the frequency of the external driving force as control parameter. Simple as this choice may seem only a few theoretical and experimental works have addressed it in the past. From this perspective, our study should stimulate further theoretical work in SR of small systems where noise intensity and thermodynamic stability are tightly coupled. Another consequence of the noise intensity vs thermodynamic stability coupling is the strong variability exhibited by single-molecule SR experiments: the measured signal-to-noise ratio versus any control parameter (in our case, oscillation frequency) will tend to show large variations from molecule to molecule. This was apparent in the results for hairpin H1 shown in Fig. 3 and has been observed in the rest of molecules (see, for instance the results shown in Fig. 7 for SH8). Such variability is consequence of the aforementioned weak stability of biomolecular bonds, and various sources of experimental errors (e.g. instrumental drift, misalignment attachment, inaccurate discrimination of the co-existence

force, etc.). It has no counterpart in other SR studies of non-linear macroscopic devices or single degree-of-freedom systems (such as single colloidal particle in optical traps or macroscopic systems in solid state physics or electronic devices).

## IX. FUTURE PERSPECTIVES

The results of our work suggest that we could extract the kinetic rates of molecular hoppers by measuring the resonance frequency in oscillating experiments. Is this approach useful? There are several widely accepted and commonly used single-molecule methods that can extract the kinetic parameters of molecular hoppers just by analyzing the hopping traces without bothering about carrying out oscillating measurements. It is then clear that single-molecule SR is not worth pursuing if other simpler methods are available. Yet SR might be of interest for investigating fast molecular transitions where current methods might fail. In Section VII, we investigated SR in an 8bp short DNA hairpin (SH8) at conditions (low trap stiffness) where hopping rates are hard to be measured from standard methods (e.g. the Bell-Evans model). The faster hopping rate and the smaller jumps in extension (due to both the shorter length of SH8 and the decreased trap stiffness) contribute to make the hopping rate measurements difficult. Note that we have been able to extract the value of the hopping rate either by measuring the power spectrum (Fig. 6b) or by implementing a hidden-Markov model. Interestingly, whereas applying standard methods to extract kinetic rates become steadily difficult as the hopping signal becomes more noisy, the quality of the resonant peak in the SNR remains acceptable (Fig. 6d). This suggests that in experimental conditions where hopping signals become nearly undetectable, SR may find a fertile ground for useful applications.

Measuring the kinetics of single bonds might be crucial to dissect the kinetic pathways of many reactions, from nucleic acid translocases indispensable in virtually all tasks of nucleic acids metabolism, to molecular folding of proteins and ligand-receptor binding. Moreover, the detection of single bond kinetics also provides a direct measurement of the affinity (or free energy of formation) of weak single bonds (e.g. important for an accurate

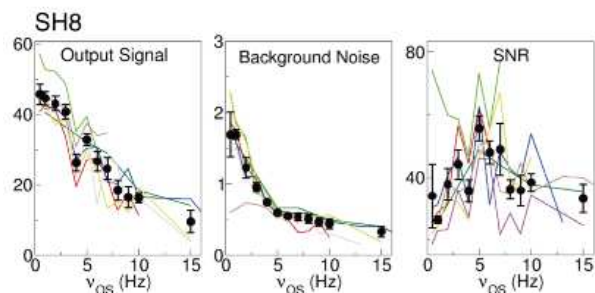


FIG. 7: **Molecular variability of the measured responses (SH8).** Results for the OS, BN and SNR for 7 different SH8 molecules. Units: OS ( $\text{nm}^2$ ), BN ( $\text{nm}^2/\text{Hz}$ ), SNR (Hz). The error bars represent the standard error over different molecules.

determination of the parameters characterizing the thermodynamics of secondary structure formation in nucleic acids [32]). It is therefore important to explore new approaches capable of illuminating into such questions. The experimental resolution of formation/dissociation kinetics is currently limited to 5 base pairs [28, 31]. Overcoming this limit strongly relies not only on increasing the hopping signal relative to the noise but also in slowing down the (expected too fast) formation/dissociation kinetics of single bonds. A direct measurement of the formation/dissociation fast kinetics of single molecular bonds stretchable along sub-nanometer scales and resistant to low (a few piconewton) forces remains an experimental challenge.

In fact, the route to discriminate hopping kinetics in a small number of base pairs may be plagued of difficulties. The situation might be even worse if the aim is to detect the unraveling kinetics of a single nearest-neighbor base pair (NNBP), which is the minimal unit of DNA bonds (double stranded helices are stabilized by both hydrogen bonds between complementary bases and stacking between NNBP). Currently most kinetics measurements are carried out in hopping experiments. However there is a complication present in hopping experiments due to the low signal-to-noise ratio inherent to unraveling a single NNBP together with the disturbances caused by the multifrequential noise present in the high frequency range where the kinetic rate of formation/dissociation of a single NNBP is expected to fall. The low signal-to-noise ratio problem can be partially resolved using advanced data analysis tools such as Bayesian methods and HMM to unravel hopping traces for SH8. However such methods assume a specific form of the noise (i.e. decorrelated force fluctuations and Gaussian emission signal) and do not account for multifrequential sources of noise (due to the aforementioned sources). In this regard, SR might be extremely useful to separate the true formation/dissociation kinetics of a single NNBP from these other artifacts.

Finally our work focused in the SR phenomenon

in DNA hairpins whereas other interesting molecular structures are now available for single molecule pulling. From this point of view, it would be very interesting to carry out SR measurements in more complex molecular folders (e.g. exhibiting multiple folding pathways, intermediate states or non-cooperative transitions) such as RNAs and proteins.

## Methods.

**Synthesis of DNA hairpins.** The DNA hairpins with handles are synthesized using the hybridization of three different oligonucleotides (Fig. 1a). One oligonucleotide contains the sequence of the ssDNA left handle plus a part of the sequence of the desired DNA hairpin; the second has the rest of the sequence of the DNA hairpin and the ssDNA right handle. The right and the left handles have the same sequence in order to hybridize them with the third oligonucleotide. The first oligonucleotide has a biotin at its 5' end and the second oligonucleotide has been modified at its 3' end with a digoxigenin tail (DIG Oligonucleotide Tailing Kit, 2nd generation, Roche Applied Science). Once the first and the second oligonucleotides are hybridized to form the hairpin, the third oligonucleotide is hybridized to the handles to form the dsDNA handles. Streptavidin-coated polystyrene microspheres ( $1.87 \mu\text{m}$ ; Spherotech, Livertyville, IL) and protein G microspheres ( $3.0\text{-}3.4 \mu\text{m}$ ; G. Kisker Gbr, Products for Biotechnology) coated with anti-digoxigenin polyclonal antibodies (Roche Applied Science) were used for specific attachments to the DNA molecular constructions described above. Attachment to the anti-digoxigenin microspheres was achieved first by incubating the beads with the tether DNA. The second attachment was achieved in the fluidics chamber and was accomplished by bringing a trapped anti-digoxigenin and streptavidin microspheres close to each other. The sequences of the short hairpins are: SH10 (5'-GCGGCGCCAGTTTTTTTTCTGGCGCCGC-3'), SH8 (5'-GGCGCCAGTTTTTTTTCTGGCGCC-3').

**Experimental setup.** The experiments have been carried out using a high stability newly designed miniaturized dual-beam optical tweezers apparatus [32]. It consists of two counter-propagating laser beams of 845 nm wavelength that form a single optical trap where particles can be trapped by gradient forces. The DNA hairpin is tethered between two beads (Fig. 1a). One bead is immobilized at the tip of a micropipette that is glued to the fluidics chamber; the optical trap captures the other bead. The light deflected by the bead is collected by two photodetectors located at opposite sides of the chamber. They directly measure the total change in light momentum which is equal to the net force acting on the bead. Piezo actuators bend the optical fibers and allow the user to move the optical trap. The force is made to oscillate using a force feedback system that operates at 4 kHz minimizing instrumental drift effects as compared to protocols without feedback. Force feedback does not introduce artifacts in our measurements unless

$\nu_{os}$  is too high (typically larger than 50 Hz) or  $A$  is too small (less than 0.1 pN).

The folding-unfolding experiments described in this report were performed at room temperature (24°C) in a buffer containing 10mM Tris-HCl pH7.5, 1mM EDTA, 1M NaCl, 0.01% Sodium Azide.

**Acknowledgements.** K. H. is supported by Grant-in-Aid for Scientific Research from the MEXT (No. 23107703). M. M. is supported by HFSP RGP0003/2007-C and EU (BioNanoSwitch). J. M. H., N. F. and F. R. are supported by grants FIS2007-3454, Icrea Academia 2008 and HFSP (RGP0055-2008).

- 
- [1] R. Benzi, A. Sutera and A. Vulpiani, *The mechanism of stochastic resonance*, J. Phys. A **14**, L453 (1981).
- [2] R. Benzi, G. Parisi, A. Sutera and A. Vulpiani, *Stochastic resonance in climatic changes*, Tellus **34**, 10 (1982).
- [3] A. Simon and A. Libchaber, *Escape and synchronization of a Brownian particle*, Phys. Rev. Lett. **68**, 3375 (1992).
- [4] C. Schmitt, B. Dybiec, P. Hänggi and C. Bechinger, *Stochastic resonance vs. resonant activation*, Europhys. Lett. **74**, 937 (2006).
- [5] P. Jop, A. Petrosyan and S. Ciliberto, *Work and dissipation fluctuations near the stochastic resonance of a colloidal particle*, Europhys. Lett. **81**, 50005 (2008).
- [6] D. F. Russell, L. A. Wilkens and F. Moss, *Use of behavioural stochastic resonance by paddle fish for feeding*, Nature **402**, 291-293 (1999).
- [7] M. McDonnell and D. Abbott, *What is stochastic resonance? Definitions, Misconceptions, debates, and its relevance to biology*, PLoS Comp. Bio. **5**, e1000348 (2009).
- [8] D. Petracchi, M. Pellegrini, M. Pellegrino, M. Barbi and F. Moss, *Periodic forcing of a  $K^+$  channel at various temperature*, Biophys. J. **66**, 1844 (1994).
- [9] M. Grifoni and P. Hänggi, *Coherent and incoherent quantum stochastic resonance*, Phys. Rev. Lett. **76**, 11 (1996).
- [10] D. Witthaut, F. Trimborn and S. Wimberger, *Dissipation-induced coherence and stochastic resonance of an open two-mode Bose-Einstein condensate*, Phys. Rev. A **79**, 033621 (2009).
- [11] L. Gammaitoni, P. Hänggi, P. Jung and F. Marchesoni, *Stochastic resonance*, Rev. Mod. Phys. **70**, 223 (1998).
- [12] T. Wellens, V. Shatokhin and A. Buchleitner, *Stochastic resonance*, Rep. Prog. Phys. **67**, 45 (2004).
- [13] N. Forns, S. de Lorenzo, M. Manosas, K. Hayashi, J. M. Huguët and F. Ritort, *Improving signal-to-noise resolution in single molecule experiments using molecular constructs with short handles*, Biophys. J. **100**, 1765 (2011).
- [14] For 29bp molecular handles ( $\approx 10$  nm of contour length at each flanking side), the molecular extension is short ( $\approx 20$ nm) and the beads are very close to each other. However the high stiffness of the handle under tension prevents the beads from clashing [13].
- [15] J-D. Wen, M. Manosas, P. T. X. Li, S. B. Smith, C. Bustamante, F. Ritort and I. Tinoco, *Force unfolding kinetics of RNA using optical tweezers. I. Effects of experimental variables on measured results*, Biophys. J. **92**, 2996 (2007).
- [16] M. Manosas, J.-D. Wen, P.T.X. Li, S.B. Smith, C. Bustamante, I. Tinoco and F. Ritort, *Force unfolding kinetics of RNA using optical tweezers. II. Modeling experiments*, Biophys. J. **92**, 3010 (2007).
- [17] B. McNamara and K. Wiesenfeld, *Theory of stochastic resonance*, Phys. Rev. A **39**, 4854 (1989).
- [18] N. G. Stocks, *A theoretical study of the non-linear response of a periodically driven bistable system*, Nuovo Cimento D **17**, 925 (1995).
- [19] A. L. Pankratov, *Suppression of noise in nonlinear systems subjected to strong periodic driving*, Phys. Rev. E **65**, 022101 (2002).
- [20] V. Berdichevsky and M. Gitterman, *Stochastic resonance in a bistable piecewise potential: analytical solution*, J. Phys. A: Math. Gen. **29**, L447 (1996).
- [21] M. C. Mahato and A. M. Jayannavar, *Some stochastic phenomena in a driven double-well system*, Physica A **248**, 138 (1998).
- [22] J. Casado-Pascual, J. Gomez-Ordoñez, M. Morillo and P. Hänggi, *Two-state theory of nonlinear stochastic resonance*, Phys. Rev. Lett. **91**, 210601 (2003).
- [23] L. Gammaitoni, F. Marchesoni and S. Santucci, *Stochastic resonance as a bona fide resonance*, Phys. Rev. Lett. **74**, 1052 (1995).
- [24] T. Zhou, F. Moss and P. Jung, *Escape-time distributions of a periodically modulated bistable system with noise*, Phys. Rev. A **42**, 3161 (1990).
- [25] S. Saika, R. Ratnadeep and A. M. Jayannavar, *Work fluctuations and stochastic resonance*, Physics Letters A **369**, 367 (2007).
- [26] A. Mossa, S. De Lorenzo, J. M. Huguët and F. Ritort, *Measurement of work in single molecule experiments*, J. Chem. Phys. **130**, 234116 (2009).
- [27] P. Jung and F. Marchesoni, *Energetics of stochastic resonance*, CHAOS **21**, 047516 (2011).
- [28] M. T. Woodside, W. M. Behnke-Parks, K. Larizadeh, K. Travers, D. Herschlag and S. M. Block, *Nanomechanical measurements of the sequence-dependent folding landscapes of single nucleic acid hairpins*, Proc. Natl. Acad. Sci. **103**, 6190 (2006).
- [29] A. Mossa, M. Manosas, N. Forns, J. M. Huguët and F. Ritort, *Dynamic force spectroscopy of DNA hairpins (I): Irreversibility and dissipation*, J. Stat. Mech., P02060 (2009).
- [30] F. E. Müllner, S. Syed, P. R. Selvin and F. J. Sigworth, *Improved hidden Markov models for molecular motors, Part 1: Basic theory*, Biophys. J. **99**, 3684 (2010).
- [31] J. M. Huguët, N. Forns and F. Ritort, *Statistical properties of metastable intermediates in DNA unzipping*, Physical Review Letters, **103** 248106 (2009).
- [32] J. M. Huguët, C. V. Bizarro, N. Forns, S. B. Smith, C. Bustamante and F. Ritort, *Single-molecule derivation of salt dependent base-pair free energies in DNA*, Proc. Natl. Acad. Sci. **107**, 15431-15436 (2010).